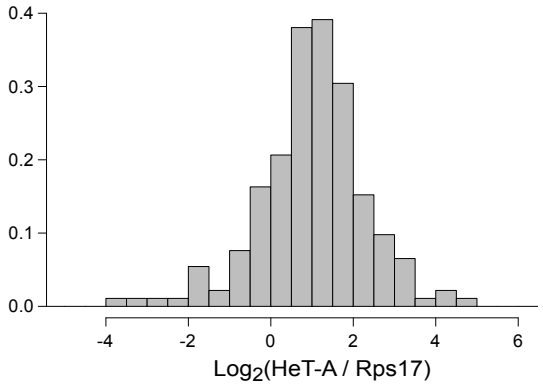

Supplementary Figure 1. Histogram of HeT-A quantities in log scale based on data from Fig. 1A.

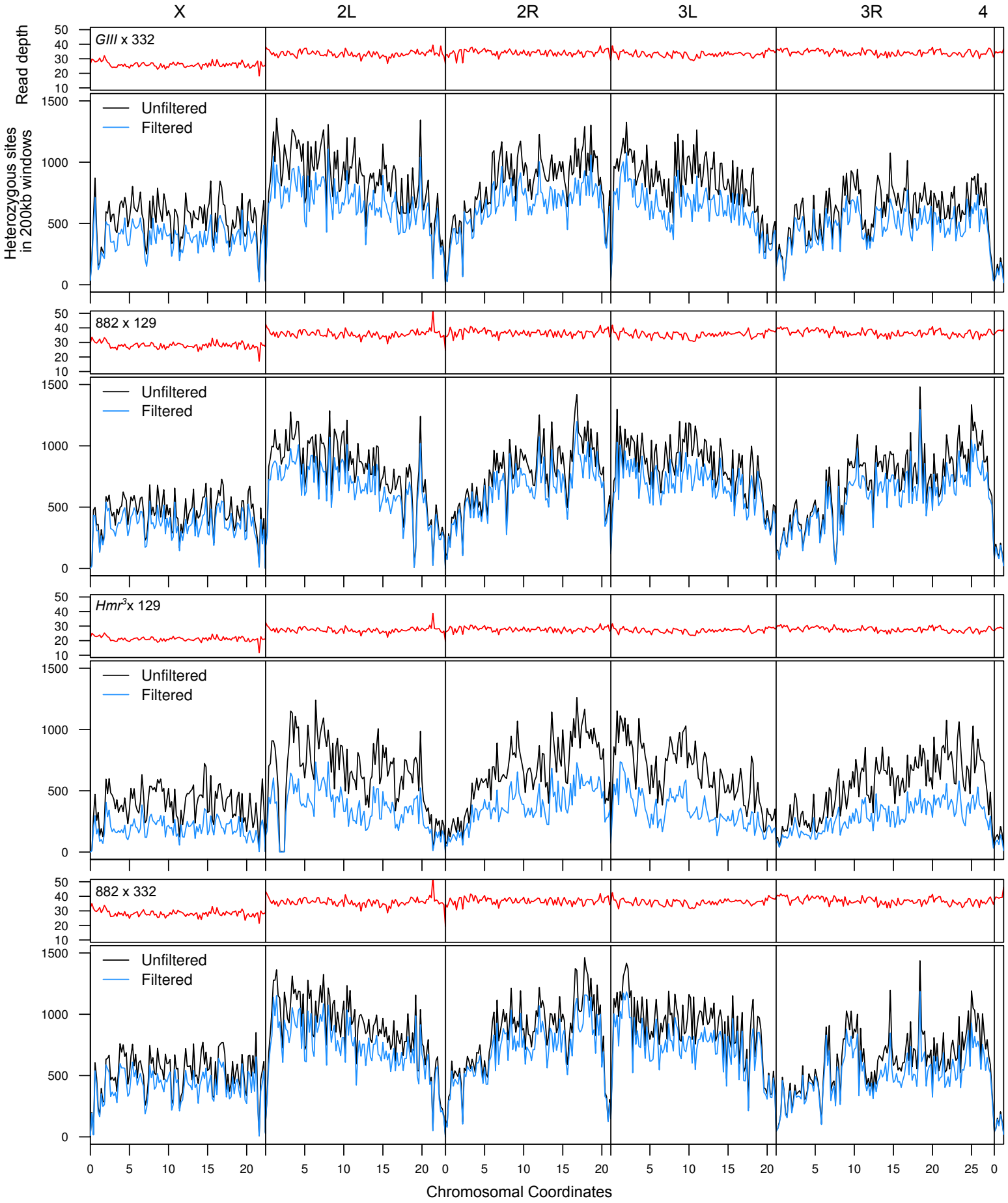

Supplementary Figure 2. Read depth and SNP density. For each of the four crosses, the read depth across the genome is plotted in the top panel, and the number of heterozygous SNPs before and after filtering by read depth in each 200kb window is plotted in the lower panel. The read-depth filter removes SNPs with read depths below 20 (X-linked) or 25 (autosomal), or above twice the average read depth.

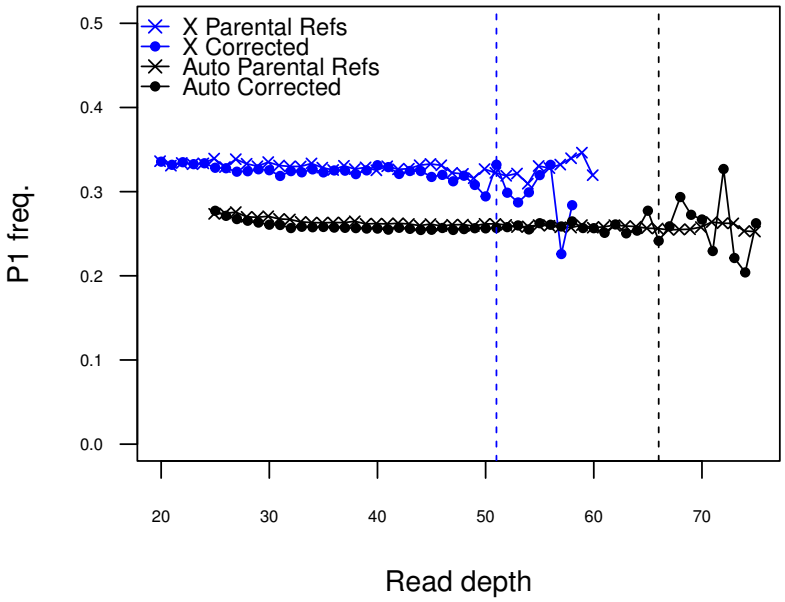

Supplementary Figure 3. Reference allele bias correction. The allele frequencies after reference allele bias correction (replotted from Figure 2C) are plotted along with allele frequencies generated from alignments to both parental genomes, an alternative strategy to minimize bias. To do this, we used GATK's Alternate Reference Maker to modify the reference genome with SNPs found in DGRP-882 or DGRP-129, generating the two parental genomes to which the DGRP-882 x DGRP-129 cross was aligned. After SNP calling with GATK, the P1 and P2 counts at each heterozygous site are simply the reference counts from the alignment to DGRP-882 and DGRP-129, respectively. The dashed vertical lines represent the upper-bound read depth cut off (twice the average read depth).

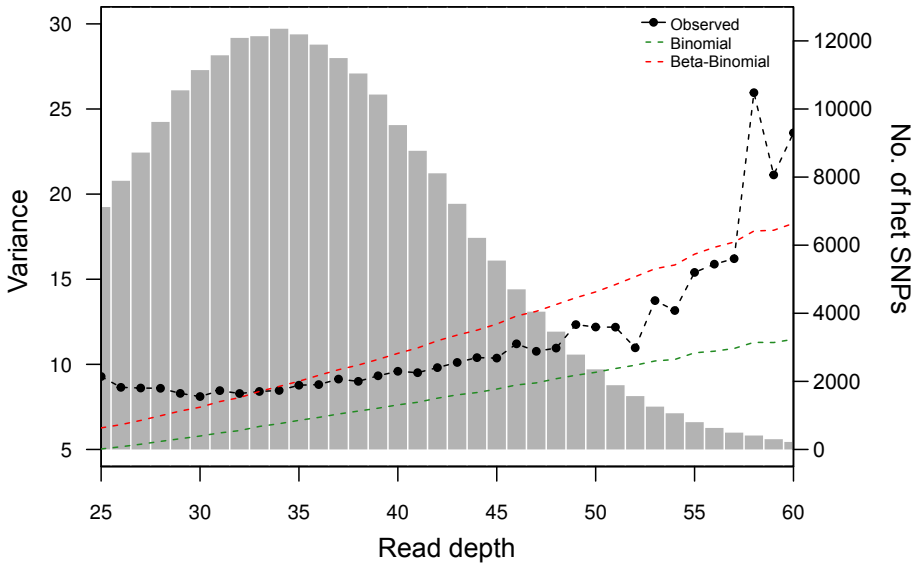

Supplementary Figure 4. Estimating and modeling variance in allele frequency. The observed variance of P1 counts at different read depth bins is plotted with black connected dots. The expected variance under Binomial (green) and Beta-Binomial (red) sampling is plotted in dotted lines. The histogram of the read depth distribution of heterozygous SNPs is plotted with gray shading in the background.

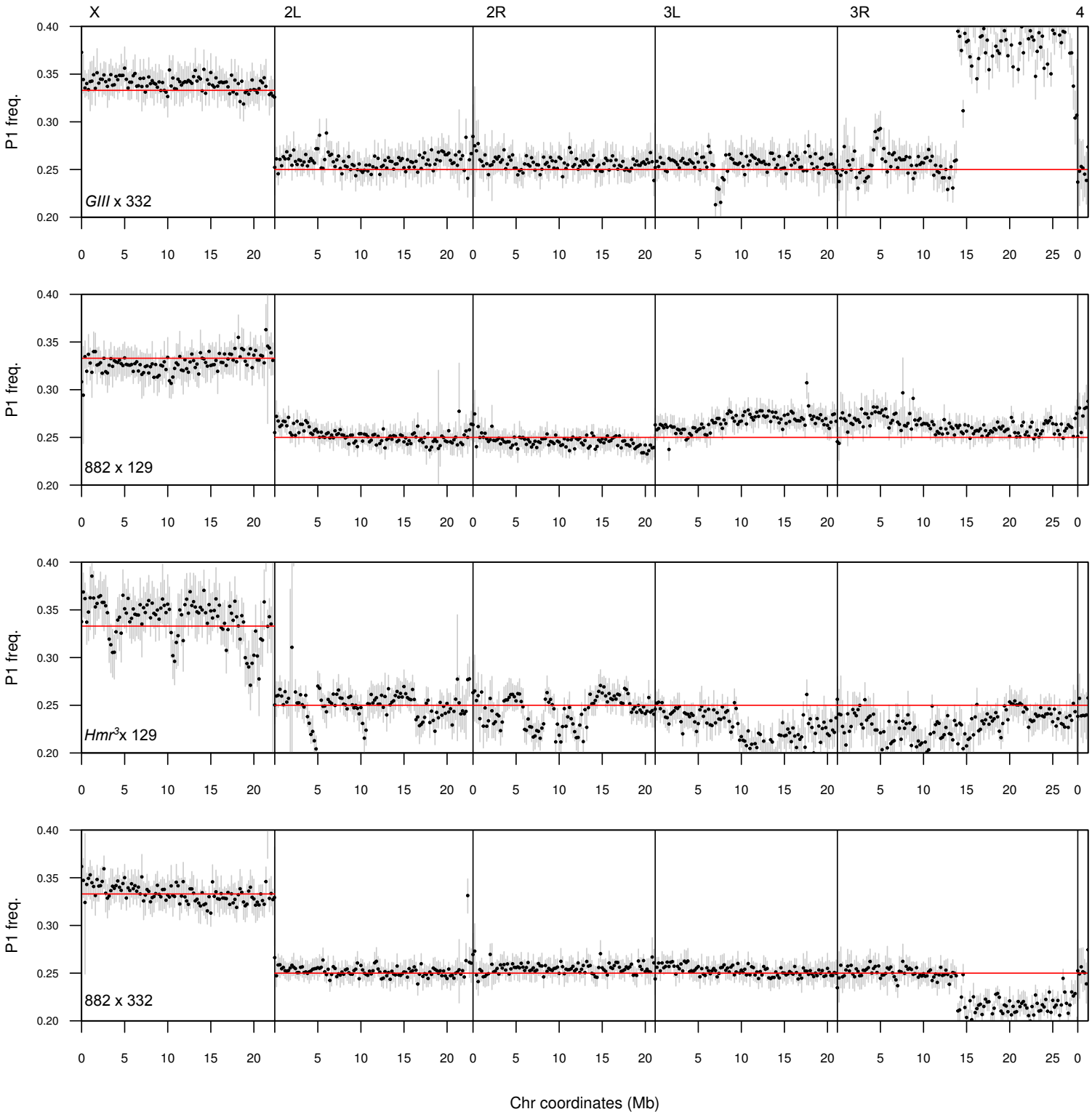

Supplementary Figure 5. Allele frequency across chromosomes after filtering out SNPs within 100bps. Because heterozygous sites that are less than 100bps apart cannot be independently sampled given 100bp reads, sites used to generate Figure 3 were further filtered to remove neighboring SNPs within 100bps. When multiple heterozygous SNP sites were found within 100bp, only one site was kept at random.

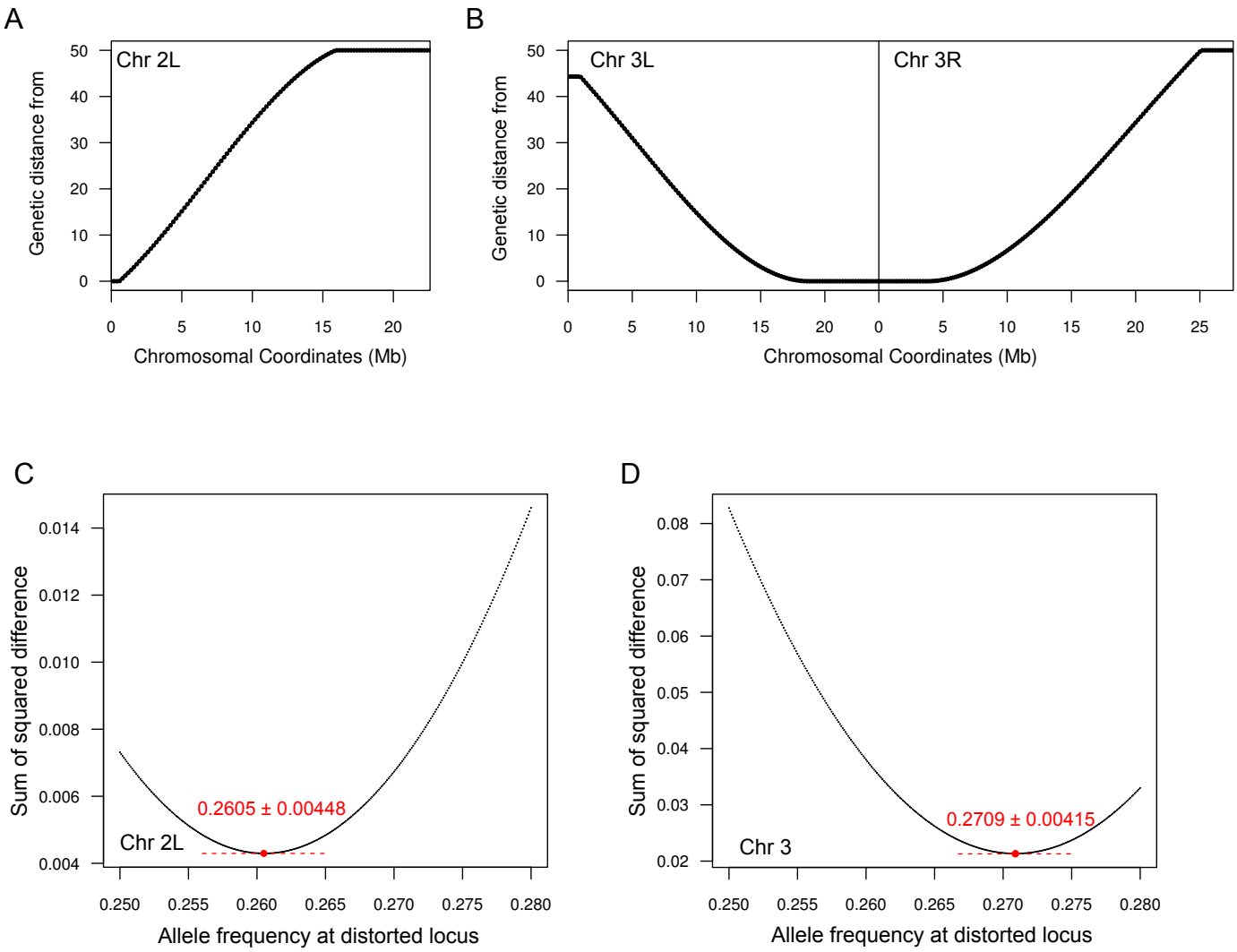

Supplementary Figure 6. Distortion estimates based on best fit to recombination decay. Genetic distance from the telomere of Chr. 2L (A) and centromere of Chr. 3 (B) is plotted. To estimate the allele frequency at the two putative distortion loci from the DGRP-882 x DGRP-129 cross in Figure 5, we determined the fit of the decay curve with distorted P1 allele frequencies increasing at 0.0001 intervals, starting at 0.25 (i.e. no distortion). The fit as determined by the sum of squared difference between the observed allele frequency at each window and the curve is plotted for each distortion allele frequency. The least square value is approximated by the lowest point (red) in the graphs. The dotted red lines demarcate the 95% confidence intervals for the least square estimates which are also noted in red above of the points. For the locus at the telomere of Chr. 2L (C), the fit was based only on chromosome arm 2L because arm 2R is unlinked from the telomere. For the locus at the centromere of Chr. 3 (D), the fit was summed over both 3L and 3R.

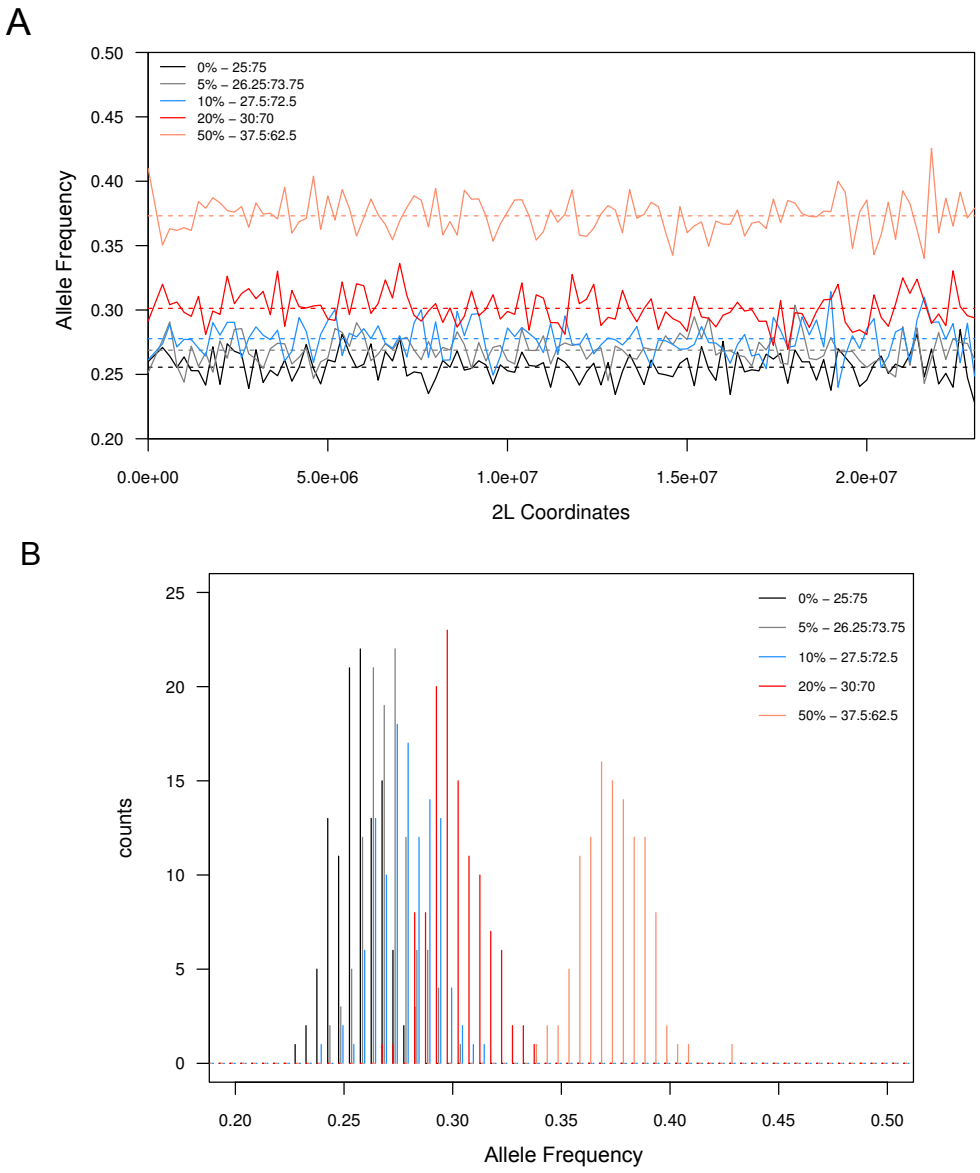

Supplementary Figure 7. Simulation of crosses with meiotic drivers of different strengths. We simulated the results of pooled sequencing by generating and concatenating simulated reads from chromosome 2L of DGRP-882 and DGRP-129 at different ratios. The reads were then mapped/processed as per our pipeline. A) With drivers of different strengths (different colors as indicated by legend), P1 allele frequencies in 200kb windows are plotted across the chromosome for one simulation each. Dotted lines indicate the average across the chromosome for each driver strength. B) Distributions of allele frequencies for all 200kb windows plotted in A) above for different meiotic driver strengths. All pair-wise comparisons of the distributions are statistically significant (Wilcoxon Ranked Test).